Reactions in Multiindexed Continuous Mixtures: Catalytic Cracking of Petroleum Fractions

F. C. Peixoto
Grupo de Química, Instituto de Pesquisa e Desenvolvimento, CTEX, Rio de Janeiro, RJ, CEP: 23020-470, Brazil

J. L. de Medeiros
Dept. de Engenharia Química, Univ. Federal do Rio de Janeiro, Centro de Tecnologia, Rio de Janeiro, RJ, CEP: 21949-900 Brazil

The classic breakage problem is a population-balance problem using first-order kinetics and product distribution rules over a multidimensional continuum, mathematically expressed as linear integrodifferential equations for the multiindexed frequency distribution functions of entities. To model the catalytic cracking of petroleum fractions, population-balance equations are solved through Galerkin formalism. It focuses on a simplified version of such equations, which was solved analytically through the method of characteristics. Kinetic and stoichiometric parameters were statistically estimated for both models from a set of pseudoexperimental data generated using available traditional lumped models. For this purpose, an arbitrary structural description for a continuous representation of the species also had to be developed.

Introduction

Catalytic cracking of petroleum fractions has been the largest and most important catalytic process in the world for a long time. This fact explains why so much research effort has been focused on explaining its complex kinetic framework—a predictive kinetic description of such processes are useful for the design, optimization, and control of commercial plants (Jacob et al., 1976). Since Voorhies (1945) first established some simple rate kinetic laws concerning the mechanisms of cracking conversion and coke formation/deposition (and, consequently, catalyst decay), several authors have tried to explain other phenomena related to catalytic cracking.

Perhaps because of the kind of chemical or physical analysis traditionally employed (such as density, average molecular weight, or refractive index), some authors were led to believe that a lumping procedure must be used to access the ten thousand or so individual chemical species present in a typical gas oil fraction (Sachanen, 1945). Correlations were then developed to predict the weight fraction of carbon atoms present in paraffinic, naphthenic, and aromatic species using the physical measurements already mentioned (Van Nes and Van Westen, 1951). Thus, the catalytic cracking of petroleum fractions have been traditionally accessed through lumped models in which pseudocomponents are chosen to characterize the whole mixture. A simple mathematical formulation is achieved and solved, but with serious restrictions with respect to physical property predictions, once they are highly dependent on the choice of the key components for each lump.

Besides, those authors began to notice that parameters adjusted for these kinds of (lumped) model tended to be highly dependent on the feedstock employed in the experiment, whose data are used in parameter regression (Jacob et al., 1976). The solution was usually the adoption of a greater number of lumps. For example, Voltz and Weekman, in Nace et al. (1971), used a 3-lump scheme, and five years later (Jacob et al., 1976), the same authors had developed an improved 10-lump structure, which also incorporated some catalyst-decay and ring-adsorption effects.

Additionally, second-order kinetics were frequently considered the best for adjusting lumped models (Ho and Aris, 1987); however, catalytic cracking of individual species is typically a first-order process. The explanation of this paradox is

Correspondence concerning this article should be addressed to F. C. Peixoto.

that the distribution of reacting species leads to an apparent reaction of order higher than one, since the reaction tends to slow down, as the more refractory species remain to be cracked (Luss and Hutchinson, 1971; Hutchinson and Luss, 1970; Aris, 1989). The solution for this problem was the creation of a fitted refractivity function (Kemp and Wojciechowski, 1974). Even some criteria for lumping species together had to be developed so as to preserve important characteristics of the reaction systems (Wei and Kuo, 1969; Ozawa, 1973).

The three previous paragraphs review the main motivations of the present continuous approach. The concept of the continuity of a given mixture is applied whenever that mixture is so complex that it is no longer worthwhile to distinguish among individual chemical species; instead, an index (such as the number of carbon atoms, boiling point, or chromatographic retention time) is chosen to characterize each component, and the continuity of this index is assumed. The molar concentration C_i of species A_i is replaced by $f(x)dx$, the molar concentration of material with an index in the $(x, x + dx)$ interval. Function $f(x)$ is known as the mixture concentration distribution function (CDF) in kgmol/m^3, where x is the continuous index of the mixture (Aris, 1989).

In some cases, more than one index must be used to completely characterize the continuum of species (for example, petroleum fractions), which increases the mathematical complexity of any phenomena described with a continuous approach. If x is a vector of continuous indexes, the CDF of the system is denoted by $f(x)$ and the molar concentration of species with indexes in the region $(x, x + \mathrm{d}x)$ is given by the analogous expression $f(x)d^n x$.

Distribution functions exhibit an obvious normalization condition given by:

$$\int_0^\infty \cdots \int_0^\infty f(x,t)\,d^n x = C(t) \qquad \int_0^\infty \cdots \int_0^\infty f0(x)\,d^n x = C0 \quad (1)$$

where $C(t)$ is the total molar concentration of the mixture at time t, $f0(x)$ is the initial CDF, and $C0$ is the initial total concentration of the mixture.

Many authors argue that the basic problem when applying a continuous description for a reactive mixture is how to find a solution for the equations involved (Liou et al., 1997; Ramkrishna, 1985). Some approximations and simplifications are commonly made in order to solve them: McCoy and coworkers (McCoy and Madras, 1997; McCoy and Wang, 1994; McCoy, 1996) adopted a domain partition and/or some particular stoichiometric coefficients and rate constants leading to certain problem simplifications; Liou et al. (1997) opted for a successive generations approach; Cicarelli et al. (1992) employed an interesting perturbation technique, but also used particular coefficients and rate constants. Some of these authors have mentioned the usage of a continuous description for catalytic cracking reactions. However, multiindexed CDFs have been avoided, probably because of the already mentioned mathematical complexity. Thus, systems that clearly needed more than one index have been approximated by more than one family of species:

$$f(x) \longrightarrow f_i(x_i) \qquad (2)$$

Additionally, some continuous descriptions of petroleum fractions (related to vapor–liquid equilibria calculations) have been conducted using inadequate continuous indexes, such as normal boiling points (Cotterman et al., 1985). This leads to a difficulty in predicting other important mixture properties, which are then accessed through empirical correlations with fitted parameters and narrow ranges of application. Peixoto et al. (2000) comprehensively addresses this problem.

This work looks at continuous modeling of the catalytic cracking of petroleum fractions, which are naturally characterized by multiindexed CDFs. Two descriptions were adopted:

(1) a multidimensional version of the fragmentation kinetics (also known as population balance or breakage equation), usually employed in comminution processes, is adopted through a warping procedure in the time scale in order to take into account catalyst deactivation effects;

(2) a simplified version of the population balance.

Both solutions were achieved and the subsequent parameter regression was conducted using pseudoexperimental lumped data. A continuous description for the gas oil was established in order to compare the continuous model outcome to the pseudoexperimental lumped data. The continuous indexes employed were chosen to be the most adequate with respect to the lumped data and to the group contribution methods used to predict physical properties.

Lumped Models for the Catalytic Cracking of Petroleum Fractions

Traditional lumped models are useful in generating pseudoexperimental data for regression of models devoted to the catalytic cracking of petroleum fractions (Jacob et al., 1976; Oliveira, 1987; Cerqueira, 1996) because:

1. They are simple, since data can be generated in any desired format. The instantaneous outlet of a cracking reactor, for instance, can be easily simulated with these models—real on line measurements are expensive and difficult to perform.

2. One can quickly (and inexpensively) generate a large amount of ''experimental'' information.

3. There are several works approaching the catalytic cracking kinetics through noncontinuous lumped models (Jacob et al., 1976; Oliveira, 1987; Cerqueira, 1996) in the literature devoted to process engineering.

4. The generation of pseudoexperimental data is a common practice when there are traditional (and reliable) models and an improvement is sought (as in the present case).

In this approach, the work of Jacob et al. (1976) deserves special attention, as it presents a 10-lump structure that has remained the most complete work on lumped kinetics for the catalytic cracking of gas oil for a long time. For our purposes, however, it has the serious disadvantage of including gaseous compounds in the same lump of coke (the *C*-lump), once we know the whole mixture volatility.

So, Oliveira's model (1987) is more appropriate, once it assumes the *C*-lump split into primary gaseous products (*Gas1*), secondary gaseous products (*Gas2*) and coke itself (*C*), besides providing more complete information on the kinetics constants involved. The reactional scheme is shown in Figure 1.

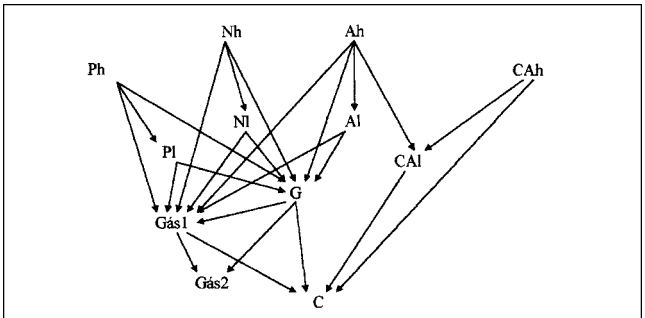

				Boiling range
a_1	- Ph	- %w/w of heavy paraffinic molecules		342°C$^+$
a_2	- Nh	- %w/w of heavy naphtenic molecules		342°C$^+$
a_3	- Ah	- %w/w of heavy aromatic substituent groups		342°C$^+$
a_4	- CAh	- %w/w of carbon atoms among aromatic rings		342°C$^+$
a_5	- Pl	- %w/w of light paraffinic molecules		216° - 342°C
a_6	- Nl	- %w/w of light naphtenic molecules		216° - 342°C
a_7	- Al	- %w/w of light aromatic substituent groups		216° - 342°C
a_8	- CAl	- %w/w of carbon atoms among aromatic rings		216° - 342°C
a_9	- G	- gasoline		C5 - 216°C
a_{10}	- Gas1	- primary gaseous products		
a_{11}	- Gas2	- secondary gaseous products		
a_{12}	- C	- coke		

Figure 1. 12-lump reactional scheme (Oliveira, 1987).

Oliveira (1987) takes adsorption dynamics into account and assumes that the deactivation phenomenon is related to the catalyst residence time (time on stream or time of experiment). Cerqueira (1996) also adopts the 12-lump scheme, but includes instantaneous adsorption and catalyst deactivation, depending on the amount of coke on the catalyst surface.

Table 1. Average Molecular Weight of Cerqueira's Lumps

MW_H	Average molecular weight of heavy lumps	370.6
MW_L	Average molecular weight of light lumps	254.7
MW_G	Average molecular weight of G lump	117.6
MW_{Gas1}	Average molecular weight of Gas1 lump	46.7
MW_{Gas2}	Average molecular weight of Gas2 lump	18.4
MW_C	Average molecular weight of C lump	400

Both models use, as experimental data, time-averaged compositions of the lumps at the end of the reactor, due to the analytical techniques employed, as described in Peixoto and de Medeiros (1999a).

Intending the construction of an experiment simulator for the reactor behavior, a hybrid model was employed using the 12-lump structure, Cerqueira's instantaneous adsorption hypothesis, and Oliveira's deactivation hypothesis:

$$\frac{da}{d\theta} = \frac{\bar{K}a}{\sum_{j=1}^{n-1} a_j} \quad \text{subject to } a(\theta = 0) = a0 \tag{3}$$

Note that, in Eq. 3, θ represents a warped time scale that takes deactivation due to nitrogen poisoning and coke deposition, and transport effects, as weight-hour space velocity and catalyst-to-oil ratio (Kobolakis and Wojciechowski, 1985; Peixoto and de Medeiros, 1999a), into account. It will always be possible to adapt such a time scale to a particular experiment using available empirical deactivation models (Oliveira, 1987; Cerqueira, 1996). This way, a computationally onerous step of numeric integration (for the calculation of the already

Table 2. Parameters for the Catalytic Cracking of Gas Oil for the 12-Lump Model

$$\bar{K} = \begin{bmatrix} -(k1+k2+k3) & 0 & 0 & 0 & 0 & 0 & 0 & 0 \\ 0 & -(k4+k5+k6) & 0 & 0 & 0 & 0 & 0 & 0 \\ 0 & 0 & -(k7+k8+k9+k10) & 0 & 0 & 0 & 0 & 0 \\ 0 & 0 & 0 & -(k11+k12) & 0 & 0 & 0 & 0 \\ \upsilon 1 * k1 & 0 & 0 & 0 & -(k13+k14) & 0 & 0 & 0 \\ 0 & \upsilon 4 * k4 & 0 & 0 & 0 & -(k15+k16) & 0 & 0 \\ 0 & 0 & \upsilon 7 * k7 & 0 & 0 & 0 & -(k17+k18) & 0 \\ 0 & 0 & \upsilon 10 * k10 & \upsilon 11 * k11 & 0 & 0 & 0 & -k19 \\ \upsilon 2 * k2 & \upsilon 6 * k6 & \upsilon 8 * k8 & 0 & \upsilon 13 * k13 & \upsilon 15 * k15 & \upsilon 17 * k17 & 0 \\ \upsilon 3 * k3 & \upsilon 5 * k5 & \upsilon 9 * k9 & 0 & \upsilon 14 * k14 & \upsilon 16 * k16 & \upsilon 18 * k18 & 0 \\ 0 & 0 & 0 & 0 & 0 & 0 & 0 & 0 \\ 0 & 0 & 0 & \upsilon 12 * k12 & 0 & 0 & 0 & \upsilon 19 * k19 \end{bmatrix}$$

$$k1 = 8.578 \times 10^3 \quad k2 = 1.754 \times 10^4 \quad k3 = 0 \quad k4 = 2.25 \times 10^4$$
$$k7 = 1.9 \times 10^4 \quad k8 = 6.3 \times 10^4 \quad k9 = 3.42 \times 10^4 \quad k10 = 5 \times 10^4$$
$$k13 = 8.307 \times 10^3 \quad k14 = 7.096 \times 10^3 \quad k15 = 6.615 \times 10^4 \quad k16 = 8.18 \times 10^3$$
$$k19 = 1 \times 10^3 \quad k20 = 2.34 \times 10^3 \quad k21 = 0 \quad k22 = 0$$

$$\upsilon 1 = \upsilon 4 = \upsilon 7 = \upsilon 10 = \upsilon 11 = MW_H/MW_L \qquad \upsilon 2 = \upsilon 6 = \upsilon 8 = MW_H/MW_G$$
$$\upsilon 14 = \upsilon 16 = \upsilon 18 = MW_L/MW_{Gas1} \qquad \upsilon 13 = \upsilon 15 = \upsilon 17 = MW_L/MW_G$$
$$\upsilon 19 = MW_L/MW_C \qquad \upsilon 22 = MW_G/MW_C$$
$$\upsilon 20 = MW_G/MW_{Gas1} \qquad \upsilon 21 = MW_G/MW_{Gas2}$$
$$\beta = 162.15 \qquad \gamma = 0.76$$

Table continued

Table 2 (Continued)

0	0	0	0
0	0	0	0
0	0	0	0
0	0	0	0
0	0	0	0
0	0	0	0
0	0	0	0
0	0	0	0
$-(k20+k21+k22)$	0	0	0
$\upsilon 20 * k20$	$-(k23+k24)$	0	0
$\upsilon 21 * k21$	$\upsilon 23 * k23$	0	0
$\upsilon 22 * k22$	$\upsilon 24 * k24$	0	0

$$k5 = 1.487\times 10^4 \qquad k6 = 8.457\times 10^4$$
$$k11 = 5.86\times 10^3 \qquad k12 = 1.463\times 10^4$$
$$k17 = 1.85\times 10^3 \qquad k18 = 3.63\times 10^3$$
$$k23 = 2.204\times 10^3 \qquad k24 = 4.88\times 10^3$$

$$\upsilon 3 = \upsilon 5 = \upsilon 9 = \mathrm{MW}_H/\mathrm{MW}_{Gas1}$$
$$\upsilon 12 = \mathrm{MW}_H/\mathrm{MW}_C$$
$$\upsilon 24 = \mathrm{MW}_{Gas1}/\mathrm{MW}_C$$
$$\upsilon 23 = \mathrm{MW}_{Gas1}/\mathrm{MW}_{Gas2}$$

Beginning of this table is on the opposite page.

mentioned time-averaged compositions at the end of the reactor) is by-passed.

Model constants are given below, where k_i represents kinetics constants (cm^3/g of catalyst-h) and υ_i represents stoichiometric coefficients calculated as average molecular weights of the lumps or relations among them. Their values depend on the basic lumps used, and for Cerqueira's lumps we have the average molecular weights in Table 1.

Parameters for the 12-lump model used for the catalytic cracking of gas oil are from the work of Cerqueira (1996), as shown in Table 2.

A typical simulation of Eq. 3 can be found in Figure 2.

Continuous 3-Dimensional Description for Gas Oil

Once species present in gas oil range from simple linear alkanes to very complex molecules with randomly distributed aromatic and naphthenic rings over its structure, an arbitrary structural description for a continuous representation of the species was established. This description was based on Quann and Jaffe's (1996) conclusions about the most common patterns of molecular structures present in petroleum and was designed to be as much compatible with the lumped kinetic framework described in the previous section as possible:

1. Paraffinic compounds and paraffinic substructures present in multifunctional compounds are preferably linear;

2. Ring compounds are mainly cata-condensed (Figure 3), which means that, at each pair of rings, an ''ascending'' displacement is observed in the aromatic and naphthenic substructures;

3. Multifunctional compounds show a single paraffinic ramification.

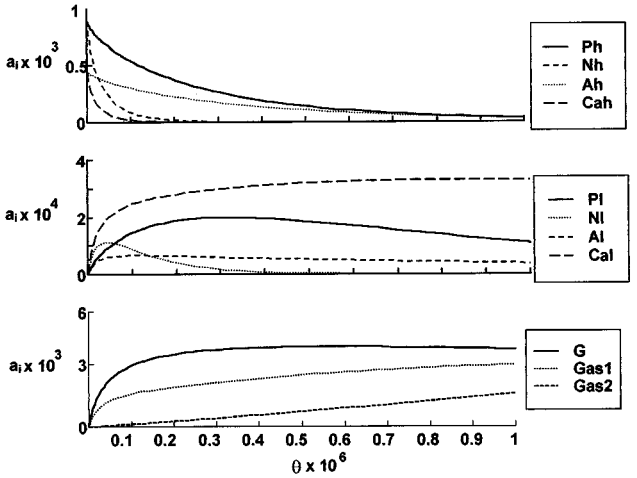

Figure 2. 12-lump model simulation.

As already mentioned, the present representation is based on admitting three types of substructures continuously present in each species: aromatic substructure, naphthenic substructure, and paraffinic substructure. Each of these substructures henceforth will be characterized by a non-negative continuous index. The connectivity among these substructures will be arbitrarily set as in Figure 4, also admitting the absence of side paraffinic ramifications.

As can be seen in Figure 4, paraffinic, naphthenic, and aromatic substructures are continuously characterized by the number of carbon atoms present in each of these substructures, designated by x, y, and z, respectively. This continuous representation was first presented in Peixoto et al. (2000), where it was used for other purposes (VLE calculations).

Applying Joback's method (Joback, 1984) to the previous continuous molecular description of the species in Figure 4, we hope to estimate thermodynamic and transport properties. With all the previous considerations, Joback's vector becomes:

$$J(x,y,z) = \begin{bmatrix} -\mathrm{CH}_3 \\ -\mathrm{CH}_2^- \\ =\mathrm{CH}-^r \\ >\mathrm{CH}_2^r \\ >\mathrm{C}=^r \\ >\mathrm{CH}-^r \end{bmatrix} = \begin{bmatrix} 1 \\ x-1 \\ 1+z/2 \\ 1+y/2 \\ -1+z/2 \\ -1+y/2 \end{bmatrix} \qquad (4)$$

where the superscript (r) indicates ring increments.

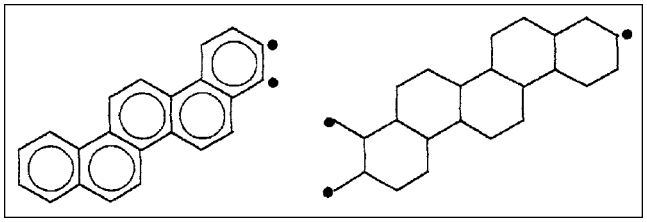

Figure 3. Cata-condensation of aromatic and naphthenic rings.

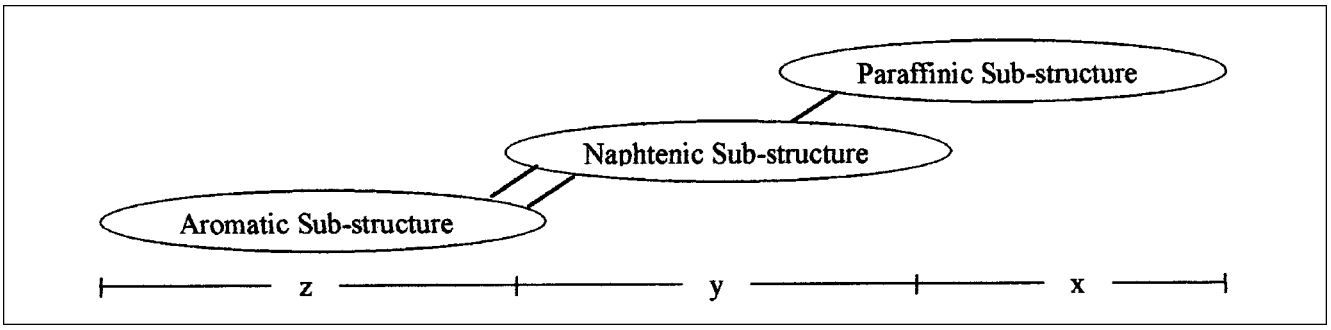

Figure 4. Connectivity among substructures of a typical molecule.

The preceding Joback representation will be satisfactory with respect to the species' chemical formulas, but will sometimes fail to correctly set the functional groups' frequencies (when one of the indexes is zero, as in an alkyl-benzene, for instance). Besides, it is an easier way to continuously describe gas-oil molecules once there are some families of species that cannot be described this way. Nevertheless, some compensation can be expected when predicting physical properties for the whole mixture.

As already mentioned, a large number of such physical properties can be accessed using this vector, for instance, normal boiling points:

$$Tb(x, y, z) = A + q_{BP}^t \cdot J(x, y, z), \tag{5}$$

with

$$q_{BP}^t = [23.58\ \ 22.88\ \ 26.73\ \ 27.15\ \ 31.01\ \ 21.78]\ \text{K/group}$$
$$\text{and}\ \ A = 198\ \text{K}. \tag{6}$$

With this property, petroleum fractions (lumps) can be continuously characterized (Figure 1). The lumping procedure then consists of integrations over compositional domains ''inside'' the regions

$$\Omega_L = \{(x, y, z) | L \le Tb \le U\}, \quad \Omega_H = \{(x, y, z) | Tb \ge U\}$$
$$\text{and}\ \ \Omega_G = \{(x, y, z) | Tb \le L\}, \tag{7}$$

where $U = 615$ K and $L = 489$ K.

In order to numerically evaluate such integrals, certain changes of variables are necessary. Each region given in Eq. 7 can be expressed using Simplex domains, due to the linear character of Eq. 5:

$$\Omega(U) = \left\{ \begin{matrix} x \,|\, Q^t \cdot x \le U \\ x \ge \mathbf{0} \end{matrix} \right\} \tag{8}$$

where $Q > \mathbf{0}$, and x, for the sake of generality, once again represents an n-dimensional vector of indexes, even though we are interested in 3-D domains (this was made to show that the present approach is able to treat higher dimensional domains). Vector Q can be algebraically obtained using Eqs. 5 and 6, and U must correspond to the region focused.

The region given by Eq. 8 corresponds to

$$0 \le x_i \le \frac{1}{Q_i}\left[U - \sum_{j=1}^{i-1} Q_j x_j\right]. \tag{9}$$

The following change of variables is defined

$$u_i \equiv \frac{x_i}{\dfrac{1}{Q_i}\left[U - \displaystyle\sum_{j=1}^{i-1} Q_j x_j\right]} \tag{10}$$

from which:

$$x_i = u_i \frac{U}{Q_i} \prod_{j=1}^{i-1} (1 - u_j) \quad \text{and} \quad 0 \le u_i \le 1. \tag{11}$$

The Jacobian matrix determinant of this application is given by:

$$\|\bar{J}\| = \|\nabla_u^t x\| = \prod_{i=1}^{n} \frac{U}{Q_i} (1 - u_i)^{n-i}. \tag{12}$$

The change of variables described in Eqs. 9 to 12, was able to turn the Simplex domain into a cubic one, as shown in Figure 5, and also allowed us to use a simple quadrature method to calculate a given property for a lump defined over one of the continuous domains in Eq. 7:

$$\int \cdots \int_{\Omega(U)} h(x)\, d^n x = \int_0^1 \cdots \int_0^1 h(x(u)) \|\bar{J}\|\, d^n u. \tag{13}$$

Thus, the Ω domains defined in Eq. 7 can be expressed in terms of Eq. 9 as

$$\Omega_H = \Omega(\infty) - \Omega(U_H) \quad \Omega_L = \Omega(U_H) - \Omega(U_L) \quad \text{and}$$
$$\Omega_G = \Omega(U_L), \tag{14}$$

with

$$U_H = 415.2 \quad Q_1 = 22.8 \quad Q_2 = 24.465 \quad Q_3 = 28.872$$
$$U_L = 16.21. \tag{15}$$

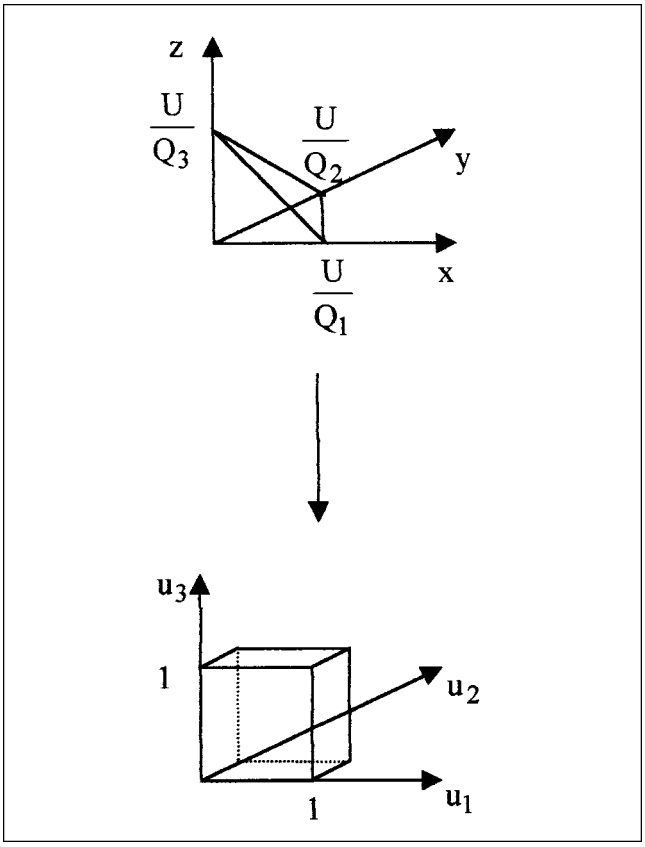

Figure 5. Change of variables.

Multiindexed Population Balance (*n*-D PB) Applied to Cracking

The process of breakage in a multiindexed continuous mixture is accessed by analogy to the one-dimensional distributed first-order fragmentation described in McCoy and and Madras (1997), McCoy and Wang (1994), McCoy (1996), Madras and McCoy (1997), Madras et al. (1997), Wang and McCoy (1995), Hill and Ng (1995, 1996), or Peixoto and de Medeiros (1999a, 1999b):

$$A(X) \xrightarrow{K(X,t)} A(X-x) + A(x), \tag{16}$$

where $A(x)$ represents an entity characterized by a vector of n continuous indexes given by x and $K(X,t)$ is a first-order kinetics constant distribution function (KCDF) for entity $A(X)$ at catalyst residence time t with units of time^{-1}.

For this kind of (multiindexed) system, the material balance applied to a mixture element with indexes in the region $[x,\ x+dx]$, traveling in a fluid element V through an isothermal heterogeneous plug-flow reactor (IHPFR), is

$$\frac{\partial}{\partial\tau}\iiint_V [\,f(x,\tau)\,d^n x\,]\,dV = \iiint_V \left[\left[-K(x,t)f(x,\tau) + \int_{x_1}^{\infty}\cdots\int_{x_n}^{\infty} K(X,t)\upsilon(x,X)f(X,\tau)\,d^n X\right] d^n x\right] dV, \tag{17}$$

where τ is the oil–catalyst contact time, and t is the catalyst residence time [time of experiment or time on stream (TOS)].

Since the previous equation is valid for any V and any x range, the kinetic equation for fragmentation without the aging or growth term, used in cell population balances (Peixoto, 2000), results, after division by $C0$;

$$\frac{\partial g(x,\tau)}{\partial\tau} = -K(x,t)g(x,\tau) + \int_{x_1}^{\infty}\cdots\int_{x_n}^{\infty} K(X,t)\upsilon(x,X)g(X,\tau)\,d^n X \tag{18}$$

subject to the initial condition:

$$g(x,0) = g0(x), \tag{19}$$

where $g0(x) = f0(x)/C0$ is the initial dimensionless concentration distribution function (IDCDF) and $g(x,\tau) = f(x,\tau)/C0$ is the dimensionless concentration distribution function (DCDF), after contact time τ with the catalyst. In the present context, $g0(x)$ represents the mixture inlet condition in the reactor, which must obey the following (obvious) normalization condition:

$$\int_0^{\infty}\cdots\int_0^{\infty} g0(x)\,d^n x = 1. \tag{20}$$

Some restrictions apply to function $\upsilon(x,X)$, the stoichiometric coefficient distribution function (SCDF). The SCDF is a distribution function of species generated after the breakage of an ancestor, and the condition concerned with its integration within the feasible index range, after the breakage of an X-indexed molecule, is

$$\int_0^{X_1}\cdots\int_0^{X_n}\upsilon(x,X)\,d^n x = 2, \tag{21}$$

since two molecules must replace a broken one (Prasad et al., 1986). Furthermore, this function must exhibit an obvious symmetry (Prasad et al., 1986), as follows:

$$\upsilon(x,X) = \upsilon(X-x,X) \tag{22}$$

It is commonly assumed that function $K(x,t)$ is a separable function of x and t (Kobolakis and Wojciechowski, 1985), as follows:

$$K(x,t) = k0K(x)D(t), \tag{23}$$

where $K(x)$ is now a dimensionless kinetic constant distribution function (DKCDF) and $k0$ is a constant or a term that is dependent on temperature and the catalyst configuration having dimension of time^{-1}. In catalytic systems, the deactivation function, $D(t)$, is the fraction of active catalytic sites after reactor run time (or catalyst residence time), t, described by

$$\frac{dD(t)}{dt} = \Im(D(t),t); \quad D(0) = 1, \tag{24}$$

where the only restriction imposed upon operator $\Im$ is that

$\Im(D(t),t)<0,\ \forall t$ as a consequence of catalyst deactivation. Following Peixoto and de Medeiros (1999a,b), Eq. 18 is divided by $k0\ D(t)$, and a warped time scale (θ) is created by the following change of variables:

$$d\theta = k0\,D(t)\,d\tau \quad \text{with} \quad \tau = 0 \rightarrow \theta = 0. \tag{25}$$

Since $\tau \ll t$ in a typical cracking run, $D(t)$ is approximately constant in $[0,\tau]$, and, therefore, Eq. 25 can be integrated over this time interval, giving:

$$\theta = k0\,D(t)\tau. \tag{26}$$

Thus, we arrive at a multiindexed version of the well-established (McCoy and Wang, 1994; McCoy, 1996; McCoy and Madras, 1997; Madras and McCoy, 1997; Madras et al., 1997; Wang and McCoy, 1995; Hill and Ng, 1995, 1996; Peixoto and de Medeiros, 1999a,b) population-balance equation of breakage (fragmentation kinetics or n-D PB), here applied to a steady-state IHPFR for catalytic cracking under catalyst deactivation

$$\frac{\partial g(x,\theta)}{\partial\theta} = -K(x)\,g(x,\theta) + \int_{x_1}^{\infty}\cdots\int_{x_n}^{\infty} K(X)\,\upsilon(x,X)\,g(X,\theta)\,d^nX, \tag{27}$$

with the following initial condition:

$$g(x,0) = g0(x); \quad \int_0^{\infty}\cdots\int_0^{\infty} g0(x)\,d^nx = 1. \tag{28}$$

When Eq. 27, subject to Eq. 28, is applied to a doubly distributed continuum, the methodology described in Prasad et al. (1986) is recovered.

So, both the continuous model (Eq. 27) and the lumped approach (Eq. 3) are solved in warped time scales, which can be forced to match using available empirical deactivation models. The discussion of such models, however, is beyond the scope of the present work, which mainly concerns the proposition of a solution to the n-D population-balance equation for breakage and its kinetic parameters regression. A detailed discussion of such empirical deactivation models can be found in Cerqueira (1996).

For the FDIAC, a product of gamma distributions with two adjustable parameters (ϵ_i and η_i) per continuous index x_i (Pearson Type III) will be employed:

$$g0(x) = \prod_{i=1}^{n} \frac{\epsilon_i^{\eta_i+1} x_i^{\eta_i} \exp(-\epsilon_i x_i)}{\Gamma(\eta_i+1)} = \prod_{i=1}^{n} g0(x_i,\epsilon_i,\eta_i). \tag{29}$$

For the DKCDF, a product of power-law functions (with adjustable parameters p) will be used:

$$K(x) = \prod_{i=1}^{n} x_i^{p_i}. \tag{30}$$

For the SCDF, the product of McCoy and Wang (1994) generalized coefficient will be used with one adjustable parameter m_i per continuous index x_i:

$$\upsilon(x,X) = B\prod_{i=1}^{n} \frac{x_i^{m_i}(X_i - x_i)^{m_i}}{X_i^{2m_i+1}} \quad \text{with} \quad B = 2\prod_{i=1}^{n} \frac{\Gamma(2m_i+2)}{\left[\Gamma(m_i+1)\right]^2}, \tag{31}$$

where B stands for Eq. 21.

Solution via Galerkin framework

An approximant form results when the DCDF is constructed as a time-dependent linear combination of linearly independent index basis functions (IBF), $\boldsymbol{\phi}(x)$, as follows:

$$g(x,\theta) = \sum_{q=1}^{\infty} c_q(\theta)\,\phi_q(x), \tag{32}$$

where the initial condition for coefficients $c_q(\theta)$ is obtained by projecting the IDCDF onto the same functional space. Equation 32 has the advantage of requiring only an analytical time integration of a linear system of differential equations after substitution in Eq. 27. Its truncation to order N leads to a matricial representation, given by

$$g(x,\theta) = \boldsymbol{\phi}^t(x)c(\theta), \tag{33}$$

where:

$$c^t(\theta) = \left[c_1(\theta)\cdots c_N(\theta)\right] \quad \text{and} \quad \boldsymbol{\phi}^t(x) = \left[\phi_1(x)\cdots\phi_N(x)\right]. \tag{34}$$

Equation 33 is then substituted in Eqs. 27 and 28, generating a residue function and its initial condition:

$$R(x,\theta) = \boldsymbol{\phi}^t(x)\dot{c}(\theta) + K(x)\boldsymbol{\phi}^t(x)c(\theta) - \int_{x_1}^{\infty}\cdots\int_{x_n}^{\infty} K(X)\upsilon(x,X)\boldsymbol{\phi}^t(X)c(\theta)d^nX \tag{35}$$

$$R(x,0) = \boldsymbol{\phi}^t(x)c(0) - g0(x). \tag{36}$$

The Galerkin method, which is an asymptotically correct method for the general solution of problems in Hilbert spaces, can be used to process such residues. It can be shown that a total basis can always be found in such spaces, which means that this basis function must be orthogonal to the residues (Kreiszig, 1978):

$$\int_0^{\infty}\cdots\int_0^{\infty} \boldsymbol{\phi}(x)\,R(x,\theta)\,d^nx = 0 \quad \text{and} \quad \int_0^{\infty}\cdots\int_0^{\infty} \boldsymbol{\phi}(x)\,R(x,0)\,d^nx = \mathbf{0}, \tag{37}$$

giving, respectively,

$$\bar{A}\cdot\dot{c}(\theta) + \bar{K}\cdot c(\theta) - \bar{D}\cdot c(\theta) = \mathbf{0} \quad \text{and} \quad \bar{A}\cdot c(0) - b = \mathbf{0}, \tag{38}$$

where

$$\bar{A} = \int_0^\infty \cdots \int_0^\infty \boldsymbol{\phi}(x)\boldsymbol{\phi}^t(x)\, d^n x,$$

$$\bar{K} = \int_0^\infty \cdots \int_0^\infty K(x)\boldsymbol{\phi}(x)\boldsymbol{\phi}^t(x)\, d^n x,$$

$$b = \int_0^\infty \cdots \int_0^\infty \boldsymbol{\phi}(x) g0(x)\, d^n x, \quad (39)$$

and

$$\bar{D} = \int_0^\infty \cdots \int_0^\infty \int_{x_1}^\infty \cdots \int_{x_n}^\infty K(X)\upsilon(x, X)\boldsymbol{\phi}(x)\boldsymbol{\phi}^t(X)\, d^n X\, d^n x. \quad (40)$$

or, by changing the order of integration in the last equation,

$$\bar{D} = \int_0^\infty \cdots \int_0^\infty \int_0^{X_1} \cdots \int_0^{X_n} K(X)\upsilon(x, X)\boldsymbol{\phi}(x)\boldsymbol{\phi}^t(X)\, d^n x\, d^n X. \quad (41)$$

In these relationships all matrices are constants of size $N \times N$. The constant vector b has size $N \times 1$.

Equations 38 are analytically solvable for the time-dependent coefficients, giving

$$c(\theta) = \exp\left(\bar{A}^{-1}(\bar{D} - \bar{K})\theta\right)\bar{A}^{-1}b. \quad (42)$$

The final form of the approximant to the DCDF is

$$g(x, \theta) = \boldsymbol{\phi}^t(x)\exp\left[\bar{A}^{-1}(D - \bar{K})\theta\right]\bar{A}^{-1}b, \quad (43)$$

which is used for simulation of the time behavior of the mixture for any choice of DKCDF $[K(x)]$, SCDF $[\upsilon(x, X)]$, IDCDF $[g0(x)]$, and IBF $[\boldsymbol{\phi}(x)]$.

Choosing the basis functions as products of unitary impulse functions, defined over the reactive continuum as

$$\phi_q(x) = \prod_{i=1}^{n} \delta(x_i - x_{i,q}), \quad (44)$$

where q is a one-to-one numbering for the nodal coordinates (x_q), we obtain

$$\bar{A} = \bar{I}, \quad \bar{K} = \text{Diag}\left[K(x_1), \ldots, K(x_N)\right], \quad \bar{D} = \overline{KVS}$$
$$\text{and} \quad b^t = \left[g0(x_1) \ldots g0(x_N)\right], \quad (45)$$

where

$$(\bar{V})_{ij} = \upsilon(x_i, x_j) \quad (46)$$

and S is the intercontribution selector matrix (ISM), given by

$$S_{ij} = \begin{cases} 1 & \text{if node } j \text{ has at least one index greater than node } i \\ 0 & \text{else.} \end{cases} \quad (47)$$

The unitary impulse functions were chosen mainly because they can treat the intercontribution (integral) portion of the equation easily. Besides, integrations in Eqs. 39 and 41 can also be easily conducted. Some other asymptotic expansions (finite-element, block-pulse, perturbation techniques, etc.) were investigated in a one-index context, and the algebra employed makes the usage of such schemes prohibitive in higher-order domains. Some other mathematical frameworks, such as, for example, moment analysis techniques (Peixoto and de Medeiros, 1999b; McCoy and Wang, 1994; McCoy, 1996; McCoy and Madras, 1997; Madras and McCoy, 1997; Madras et al., 1997; Wang and McCoy, 1995), have the advantage of being related to some physical aspects of the mixture, which, unfortunately, is not the case of the present unit impulse expansion, which is merely a mathematical tool.

The following models were developed with Eqs. 29, 30 and 31 for the IDCDF, DKCDF, and SCDF.

Simulations

In order to test the solution technique, we begin by limiting the number of continuous indexes to 3, once we are interested in the catalytic cracking of gas oil (a mixture that can be characterized by three indexes, as already shown). Simulations are then performed, employing arbitrarily chosen values for model parameters: $\epsilon x = \epsilon y = \epsilon z = 1$, $\eta x = \eta y = \eta z = 10$, $px = mx = py = my = pz = mz = k0 = 1$, and warped simulation times given by $\theta = 0$, 2×10^{-3}, 4×10^{-3}, 6×10^{-3}, 8×10^{-3}, and 10^{-2}, shown sequentially in Figure 6.

The pictorial representation is limited by the fact that four coordinates would be necessary: three indexes and the DCDF itself. So, a size scale was created, in which the DCDF value in each node is proportional to the size of the spot on its (x, y, z) coordinate. A small spot on the (x, y, z) node characterizes the absence or trace concentrations of the corresponding entity.

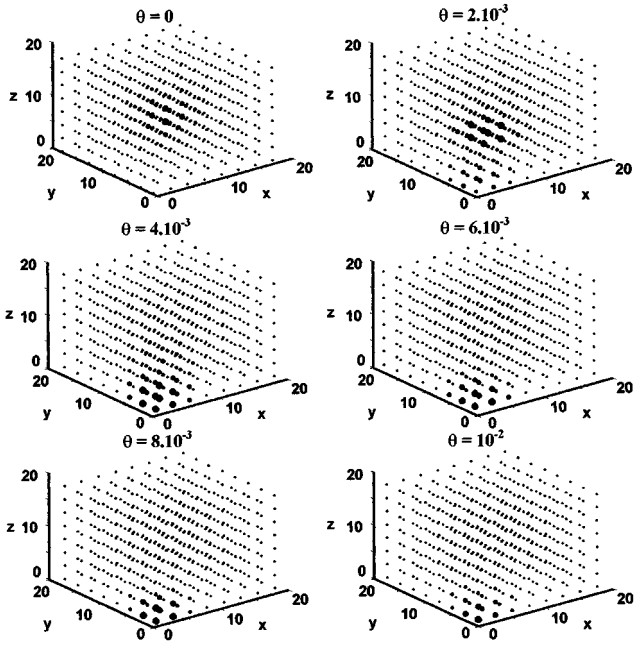

Figure 6. PB model simulation.

It can be seen in Figure 6 that the model is physically consistent, once there is an increase in the relative number of lighter species (large spots are migrating to smaller index values), which shows that the molecules are breaking up.

Multiindexed Simplified Population Balance (*n-D* SPB) Applied to Cracking

The fragmentation problem of a continuous mixture can be appreciated within a simplified multiindexed (multidimensional) population-balance context. It is an alternative approach that brings relevant results in spite of its relative mathematical simplicity. The formulation of models through simplified population-balance concepts finds application when a population can be described by one (or more) continuous parameter(s) that varies(vary) with time at a rate or velocity that is a function of this (these) parameter(s). This is the case, for instance, of crystal size in a crystal-growing population during a crystallization operation, or fluid-drop diameter in a drop-growing population during a coalescence process.

In the present approach, the population is constituted of the continuum of reactive species, with distribution related to the vector of indexes x. The kinetics or rate of population transformation will be denoted by $K(x,t)$, where this transformation is modeled by a continuous ''chemical reaction'' such that the species ''break'' continuously as:

$$A(x) \xrightarrow{K(x,t)} A(x-\Delta x)\begin{cases}\Delta x \to \mathbf{0}\\ x \geq \mathbf{0},\end{cases} \tag{48}$$

where $A(x)$ and $K(x,t)$ are defined as in Eq. 16.

Once again, the population balance inside a fluid element ΔV is carried out in the time interval $(\tau,\ \tau+\Delta\tau)$:

$$\{g(x,\tau+\Delta\tau)-g(x,\tau)\}\Delta V\prod_{i=1}^{n}\Delta x_i = \left\{\sum_{i=1}^{n} g\left(x_{j\neq i}, x_i+\Delta x_i,\tau\right)K_i\left(x_{j\neq i}, x_i+\Delta x_i,t\right)\prod_{\substack{j=1\\ j\neq i}}^{n}\Delta x_j - \sum_{i=1}^{n} g(x,\tau)K_i(x,t)\prod_{\substack{j=1\\ j\neq i}}^{n}\Delta x_j\right\}\Delta\tau\Delta V, \tag{49}$$

making $\Delta\tau\to 0$ and $\Delta x_i\to 0$ $(\forall i)$; one can find the *n-D* SPB equation, which is similar to the one in Tsang and Rao (1990),

$$\frac{\partial g(x,\theta)}{\partial\theta} = \nabla^t\cdot\left[K(x)g(x,\theta)\right] \quad \text{subject to } g(x,0)=g0(x), \tag{50}$$

where this time the time scale was warped by

$$\theta = D(t)\tau, \tag{51}$$

which is similar to Eq. 26.

Solution via the method of characteristics

A model for the KCDF, similar to Eq. 30, is proposed:

$$(K(x))_i = K_i x_i^{p_i}. \tag{52}$$

Using the method of characteristics with the following change in variables:

$$u_i(x_i,\theta) = \frac{x_i^{1-p_i}}{p_i-1} - K_i\theta \qquad i=1,\ldots,n \tag{53}$$

$$q(\theta)=\theta \tag{54}$$

we are left with the solution:

$$g(x,\theta) = g0(\aleph)\prod_{i=1}^{n}\left(\frac{\aleph_i}{x_i}\right)^{p_i}, \tag{55}$$

where

$$\aleph_i = \left[x_i^{1-p_i} - K_i\cdot(p_i-1)\cdot\theta\right]^{1/(1-p_i)} \to \lim_{n_i\to 1}\aleph_i = x_i\cdot\exp(K_i\cdot\theta). \tag{56}$$

A remark must be made on this KCDF model: it can be used in a form that takes some intercontribution among different indexes into account (in the case of some structural hindrance, for instance). However, this procedure was considered superfluous for our goal.

Simulations

Once again, the number of continuous indexes was restricted to 3, and simulations were conducted using arbitrarily chosen values for the parameters $\epsilon x=\epsilon y=\epsilon z=1$, $\eta x=\eta y=\eta z=10$, $px=Kx=py=Ky=pz=Kz=1$, and simulation warped times given by $\theta=0$, 0.2, 0.4, 0.6, 0.8, and 1.0, shown sequentially in Figure 7, using the already mentioned size scale.

Initial Distribution Parameters Calculation (ϵx, ϵy, ϵz, ηx, ηy, and ηz)

As already said, for a 3-D continuum, the model chosen for the IDCDF (Eq. 29) exhibits six adjustable parameters (ϵx, ϵy, ϵz, ηx, ηy, and ηz). However, typical gas-oil feedstocks have only six continuously distinguishable lumps—*Ph*, *Nh*, $(Ah+CAh)$, *Pl*, *Nl*, and $(Al+CAl)$—once *Ah* and *CAh*, as well as *Al* and *CAl*, cannot be considered separately in a continuous approach. So, there is not an ''excess'' of experimental data for the application of a statistical procedure of regression. The parameters are then calculated (not estimated) by a nonlinear system of equations.

In that system, pseudoexperimental data of the feedstock lumped compositions ($a0_i$ in moles of lump *i*/*g* of gas) are compared to the continuous model (Eq. 29), after expressing the pseudoexperimental data as mass fractions:

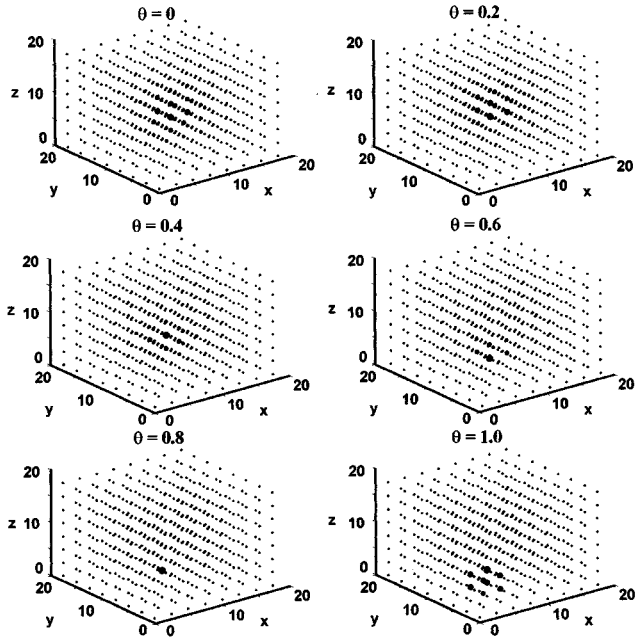

Figure 7. SPB model simulation.

$$xm0_i = \frac{a0_i \mathrm{MW}_i}{\sum_{j=1}^{n-1} a0_j \mathrm{MW}_j}, \tag{57}$$

where MW_i is the molecular weight of lump i, given in Table 1.

On the other hand, analogous auxiliary functions are created:

$$X0_i(x, y, z) = \frac{g0(x, y, z)\mathrm{mw}_i(x, y, z)}{\iiint_{\Omega(\infty)} g0(x, y, z)\mathrm{mw}_i(x, y, z)\, dx dy dz} \tag{58}$$

$$Z0_i(\Omega_j) = \iiint_{\Omega_j} X0_i(x, y, z)\, dx\, dy\, dz, \tag{59}$$

where $i = 1$ corresponds to paraffinic lumps (P); $i = 2$ to naphthenic lumps (N), $i = 3$ to aromatic lumps (A); $j = 1$ to heavy lumps (h); and $j = 2$ to light lumps (l), once, in typical feedstocks, lumps G, *Gas1* and *Gas2* are not present.

Additionally, we write molecular weight generating functions for each molecular substructure:

$$\mathrm{mw}_1(x, y, z) = \mathrm{mw}_P(x, y, z) = 14x + 1 \tag{60}$$

$$\mathrm{mw}_2(x, y, z) = \mathrm{mw}_N(x, y, z) = \frac{27}{2}y + 1 \tag{61}$$

$$\mathrm{mw}_3(x, y, z) = \mathrm{mw}_A(x, y, z) = \frac{25}{2}z + 1, \tag{62}$$

with $\Omega_1 = \Omega_H$ and $\Omega_2 = \Omega_L$ calculated as in Eq. 14.

The final system of equations for the calculation of IDCDF parameters is

Table 3. Cerqueira's Feedstock Composition

Lump	Mass Fraction
Ph	$x0m_{Ph} = 0.1720$
Nh	$x0m_{Nh} = 0.2015$
Ah + *CAh*	$x0m_{Ah} + x0m_{CAh} = 0.3735$
Pl	$x0m_{Pl} = 0.1376$
Nl	$x0m_{Nl} = 0.0860$
Al + *CAl*	$x0m_{Al} + x0m_{CAl} = 0.0294$

$$\begin{cases} Z0_P(\Omega_H) = x0m_{Ph} \\ Z0_N(\Omega_H) = x0m_{Nh} \\ Z0_A(\Omega_H) = x0m_{Ah} + x0m_{CAh} \\ Z0_P(\Omega_L) = x0m_{Pl} \\ Z0_N(\Omega_L) = x0m_{Nl} \\ Z0_A(\Omega_L) = x0m_{Al} + x0m_{CAl} \end{cases} \tag{63}$$

which is calculated employing Cerqueira's (1996) feedstock, whose composition is given in Table 3.

Using the Newton-Raphson method in Eq. 63, the result is calculated IDCDP parameters for Cerqueira's feedstock (Table 4).

SPB Kinetic Parameters Regression (*Kx*, *px*, *Ky*, *py*, *Kz*, *pz*)

As already mentioned, the usage of traditional lumped models allows the generation of a large number of pseudoexperimental data. This way, a traditional procedure of parameter regression in nonlinear models based on maximum-likelihood criteria can be employed (Britt and Luecke, 1973). Several nonlinear optimization algorithms can be used to access such regressions, but we opted for a BFGS quasi-Newton method with a mixed quadratic and cubic line search procedure (Edgar and Himmelblau, 1988).

First, pseudoexperimental data of lumped compositions are transformed into mass fractions:

$$xm_i(\theta_j) = \frac{a_i(\theta_j)\, PM_i}{\sum_{k=1}^{n-1} a_k(\theta_j)\, PM_k} \tag{64}$$

where $a_i(\theta_j)$ (in moles of /g of gas) values are found using Eq. 3.

Once more, auxiliary functions are created:

$$X(x, y, z, \theta) = \frac{g(x, y, z, \theta)\mathrm{mw}(x, y, z)}{\iiint_{\Omega(\infty)} g(x, y, z, \theta)\mathrm{mw}(x, y, z)\, dz dy dz} \tag{65}$$

$$Z_i(\Omega_j) = \iiint_{\Omega_j} X(x, y, z, \theta_i)\, dx dy dz, \tag{66}$$

Table 4. Calculated IDCDF Parameters for Cerqueira's Feedstock

$\eta x = 69.4008$	$\epsilon x = 12.0933$
$\eta y = 30.1851$	$\epsilon y = 5.0190$
$\eta z = 0.0457$	$\epsilon z = 0.1163$

Table 5. Results of the SPB Kinetic Parameters Regression

$\hat{p}x = 2.4928$	$\hat{p}y = 1.4682 \times 10^{-6}$	$\hat{p}z = 0.2375$
$\hat{K}x = 7.4933 \times 10^{4}$	$\hat{K}y = 3.6182 \times 10^{7}$	$\hat{K}z = 2.8565 \times 10^{8}$
	$S^2 = 0.9027$	

$$\overline{COV}\left(\begin{bmatrix} \hat{p}x \\ \hat{K}x \\ \hat{p}y \\ \hat{K}y \\ \hat{p}z \\ \hat{K}z \end{bmatrix}\right) = \begin{bmatrix} 0.0000 & 0.0000 & 0.0000 & 0.0000 & 0.0000 & 0.0000 \\ 0.0000 & 0.0000 & 0.0000 & -0.0002 & 0.0000 & -0.0011 \\ 0.0000 & 0.0000 & 0.0000 & 0.0000 & 0.0000 & 0.0000 \\ 0.0000 & -0.0002 & 0.0000 & 0.1092 & 0.0000 & 0.2377 \\ 0.0000 & 0.0000 & 0.0000 & 0.0000 & 0.0000 & 0.0000 \\ 0.0000 & -0.0011 & 0.0000 & 0.2377 & 0.0000 & 1.1367 \end{bmatrix}$$

where $\mathrm{mw}(x, y, z)$, the molecular weight of a molecule characterized by (x, y, z), is given by:

$$\mathrm{mw}(x, y, z) = [15\ 14\ 13\ 14\ 12\ 13] \cdot J(x, y, z) \quad (67)$$

and $g(x, y, z, \theta)$ is the model outcome (Eq. 55), $j = 1$ corresponds to heavy lumps (h), $j = 2$ to light lumps (l), and $j = 3$ to lumps *G*, *Gas1*, and *Gas2*.

It must be said that the regression was conducted by comparing heavy ($H = Ph + Nh + Ah + CAh$), light ($L = Pl + Nl + Al + CAl$), and *G* ($G + Gas1 + Gas2$) pseudoexperimental mass fractions to their continuous equivalents (Eq. 66). This regression was made to minimize the computational load and was based on the fact that it is reasonable to suppose that the distribution of the components among paraffinic (P), naphthenic (N), and aromatic ($A + CA$) lumps should always resemble the one given by the calculated IDCDF (Jacob et al., 1976).

Results are presented in Table 5, where S^2 represents an estimated variance for the model, and $\overline{COV}$ represents parameters variance–covariance matrix. Three of the fifteen 2-D projections of the confidence region are depicted in Figure 8.

As can be seen in Figure 8 and Table 4, the model exhibits a high level of confidence (high confidence for *pz*, *Kx*, *Kz*, and *Ky*) and a low variance estimate, which must be considered in addition to the good adherence to experimental data shown in Figure 9.

PB Kinetic Parameters Regression (*px*, *mx*, *py*, *my*, *pz*, *mz*, *k*0)

Once the SPB model was considered good enough for a continuous description of gas oil cracking (Figure 9), it was used as a substitute for the lumped model. Due to its higher character for a continuous approach, it was preferred for a new generation of pseudoexperimental data for the regression of PB model parameters. Once again, this was made to minimize the computational load, because if lumped data were used for this regression, the numerical integrations present in Eqs. 65 and 66 would demand several interpolations in Eq. 43.

So, the new pseudoexperimental data become:

$$y_{ij}^{\exp} = g^{\mathrm{SPB}}(x_i, \theta_j), \quad (68)$$

where g^{SPB} is the value of the SPB model (Eq. 55) calculated in x_i, the nodal coordinates used in the PB model at time θ_j. The PB model (to be adjusted) is expressed by

$$y_{ij}^{\mathrm{calc}} = c_i(\theta_j), \quad (69)$$

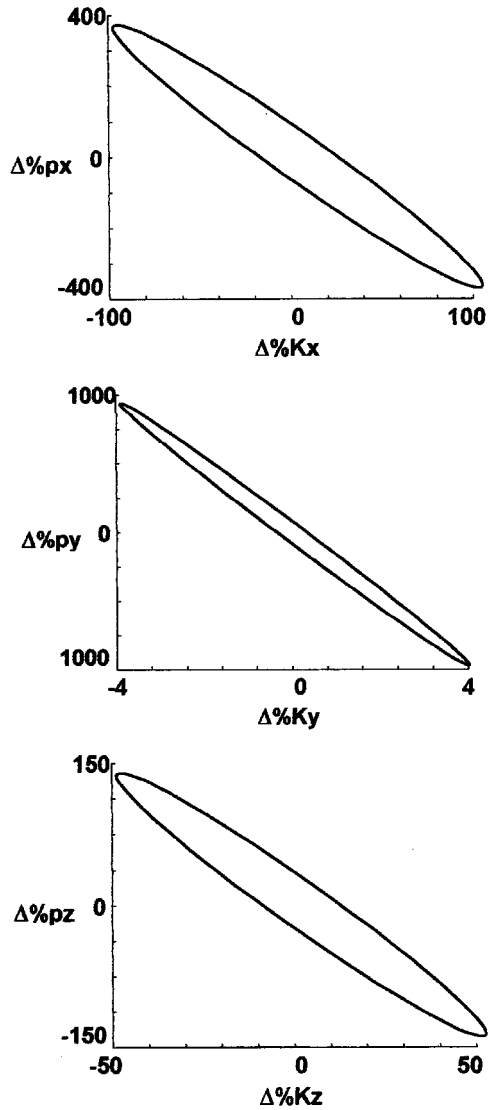

Figure 8. Confidence region projections for the SPB model.

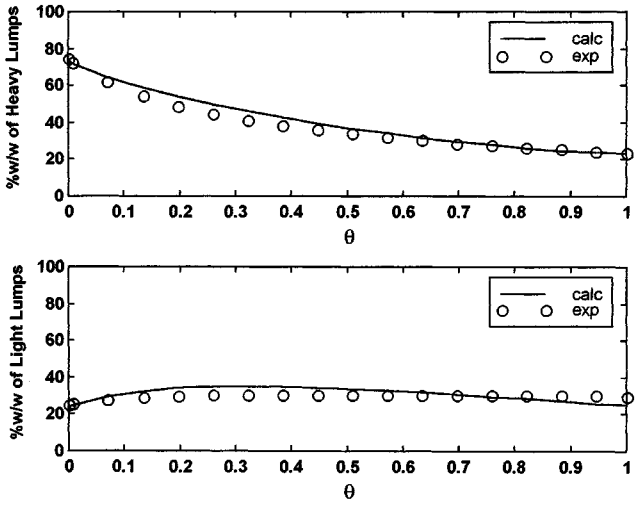

Figure 9. Fitted SPB model.

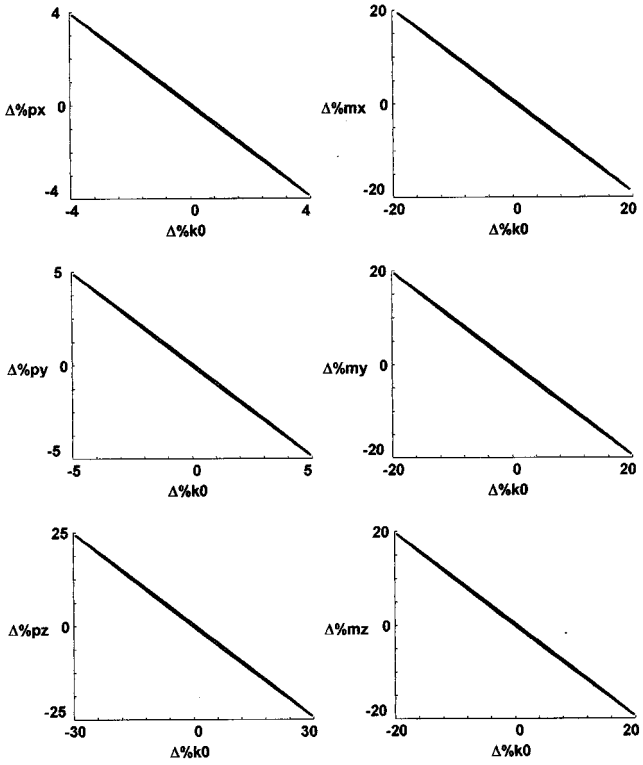

Figure 10. Some confidence region projections for the PB model.

where $c_i(\theta_j)$ is the PB model outcome for the time-dependent nodal values.

Results are presented in Table 6 and Figures 10 and 11 in a way similar to the one used for the SPB model. As can be seen in Table 5, the PB model exhibits an even lower variance estimate, probably due to the more suitable character of the data employed (continuous information). The apparent high variance of $k0$ is due to the order of magnitude of the entity itself (≈ 900).

Figure 10 shows that the model exhibits a high level of confidence and that the parameters (even though with low covariances) are slightly correlated (sharp ellipses). The adherence to the new experimental data of the present model is shown in Figure 11.

Conclusion

In this work, the multiindexed cracking problem (multidimensional population balance: *n-D* PB) was formulated within the context of catalytic cracking of a multiindexed continuous family of substances typically found in petroleum fractions, comprising generalized functions for the first-order kinetic rate and stoichiometric coefficient distribution as proposed by McCoy and Wang (1994). The governing equation was numerically solved by an asymptotically correct procedure based on a Galerkin framework and unit impulse basis functions. A simplified version of the multidimensional population-balance problem (*n*-D SPB) started with a partial first-order differential equation for the DCDF, which was solved analytically through the method of characteristics. The central object in both formulations was the dimensionless concentration distribution function of species (DCDF).

Kinetic and stoichiometric (the latter for the PB model) parameters were statistically estimated from a set of pseudo-experimental data on catalytic cracking of petroleum fractions using available traditional lumped models, reporting the instantaneous compositional distribution at the reactor outlet. Both models showed good adherence to data and good statistical properties associated to the estimates: low variance estimates (0.9027 for SPB and 2×10^{-8} for PB); and modest projections of the parameter confidence region (less than 50% amplitude for the PB model).

A final comment concerning the relative performance of these models: Probably the PB model has a better conceptual foundation, but its solution involves truncations and numerical procedures that can be too difficult in terms of computational load precluding, for example, its application in higher

Table 6. Results of the PB Kinetic Parameters Regression

$\hat{p}x = 3.1115$	$\hat{m}x = 1.0144$	$\hat{p}y = 2.8278$	$\hat{m}y = 1.0026$
$\hat{p}z = 0.1643$	$\hat{m}z = 0.9999$	$\hat{k}0 = 892.8334$	$S^2 = 1.9998\times10^{-8}$

$$\overline{COV}\left(\begin{bmatrix}\hat{n}x\\ \hat{m}x\\ \hat{n}y\\ \hat{m}y\\ \hat{n}z\\ \hat{m}z\\ \hat{k}0\end{bmatrix}\right) = \begin{bmatrix} 0.0000 & 0.0000 & 0.0000 & 0.0000 & 0.0000 & 0.0000 & -0.0013\\ 0.0000 & 0.0001 & 0.0000 & 0.0000 & 0.0000 & 0.0000 & -0.0084\\ 0.0000 & 0.0000 & 0.0000 & 0.0000 & 0.0000 & 0.0000 & 0.0000\\ 0.0000 & 0.0000 & 0.0000 & 0.0000 & 0.0000 & 0.0000 & -0.0005\\ 0.0000 & 0.0000 & 0.0000 & 0.0000 & 0.0000 & 0.0000 & 0.0013\\ 0.0000 & 0.0000 & 0.0000 & 0.0000 & 0.0000 & 0.0000 & 0.0069\\ -0.0013 & -0.0084 & 0.0000 & -0.0005 & 0.0000 & 0.0069 & 2.0642 \end{bmatrix}$$

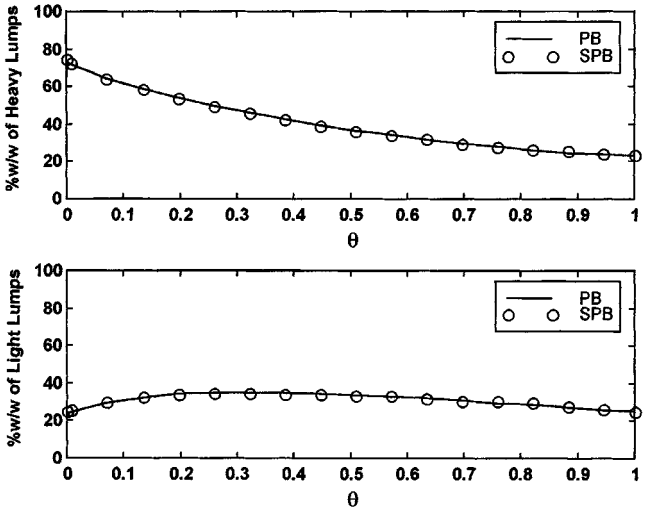

Figure 11. Fitted PB model.

dimensional index contexts. On the other hand, in spite of its simplicity and closed-form structure, the SPB performed very well, strongly suggesting its adoption in more general problems, as in a multifamily scheme and/or in higher dimensional index domains.

It must be said that the present work is part of an effort to show how useful the multiindexed context can be to the continuous approach in models devoted to petroleum processing engineering. Such formulations were shown in Peixoto et al. (2000) to be pertinent, for example, in vapor–liquid equilibria calculations; other fields of application (in areas related to petroleum refining), such as process synthesis and analysis, are under investigation.

Literature Cited

Aris, R., "Reactions in Continuous Mixtures," *AIChE J.*, **35**, 539 (1989).

Britt, H. I., and R. H. Luecke, "The Estimation of Parameters in Nonlinear, Implicit Models," *Technometrics*, **15**, 233 (1973).

Cerqueira, H. S., "Modelageme Simulação do Craqueamento Catalítico de Gasóleo em Leito Fixo: Formação de Coque," M.Sc. Thesis (in Portuguese), Universidade Federal do Rio de Janeiro, Brazil (1996).

Cicarelli, P., G. Astarita, and A. Gallifuoco, "Continuous Kinetics Lumping of Catalytic Cracking Processes," *AIChE J.*, **38**, 1038 (1992).

Cotterman, R. L., R. Bender, and J. M. Prausnitz, "Phase Equilibria for Mixtures Containing Very Many Components. Development and Application of a Continuous Thermodynamics for Chemical Process Design," *Ind. Eng. Chem. Proc. Des. Dev.*, **24**, 194 (1985).

Edgar, T. F., and D. M. Himmelblau, *Optimization of Chemical Processes*, McGraw Hill, New York (1988).

Hill, P. J., and K. M. Ng, "New Discretization Procedure for the Breakage Equation," *AIChE J.*, **41**, 1204 (1995).

Hill, P. J., and K. M. Ng, "Statistical of Multiple Particle Breakage," *AIChE J.*, **42**, 1600 (1996).

Ho, T. C., and R. Aris, "On Apparent Second-Order Kinetics," *AIChE J.*, **33**, 1050 (1987).

Hutchinson, P., and D. Luss, "Lumping of Mixtures with Many Parallel First Order Reactions," *Chem. Eng. J.*, **1**, 129 (1970).

Jacob, S. M., B. Gross, S. E. Voltz, and V. W. Weekman, "A Lumping and Reaction Scheme for Catalytic Cracking," *AIChE J.*, **22**, 701 (1976).

Joback, K. G., SM Thesis in Chemical Engineering, Massachusetts Insitute of Technology, Cambridge (1984).

Liou, J. J., S. Friedrich, and A. G. Friedrickson, "Solutions of Population Balance Models Based on a Successive Generations Approach," *Chem Eng. Sci.*, **52**, 1529 (1997).

Luss, D., and P. Hutchinson, "Lumping of Mixtures with Many Parallel N-th Order Reactions," *Chem. Eng. J.*, **2**, 172 (1971).

Kemp, R. R. D., and B. W. Wojeiechowski, "The Kinetics of Mixed Feed Reactions," *Ind. Eng. Chem. Fundam.*, **13**, 332 (1974).

Kobolakis, I., and B. W. Wojciechowski, "The Catalytic Cracking of a Fisher-Tropsch Synthesis Product," *Can. J. Chem. Eng.*, **63**, 269 (1985).

Kreyszig, E., *Introductory Functional Analysis with Applications*, Wiley, New York (1978).

Madras, G., and B. J. McCoy, "Oxidative Degradation Kinetics of Polystyrene in Solution," *Ind. Eng. Chem. Res.*, **52**, 2707 (1997).

Madras, G., G. Y. Chung, J. M. Smith, and B. J. McCoy, "Molecular Weight Effect on the Dynamics of Polystyrene Degradation," *Ind. Eng. Chem. Res.*, **36**, 2019 (1997).

McCoy, B. J., and G. Madras, "Degradation Kinetics of Polymers in Solution: Dynamics of Molecular Weight Distributions," *AIChE J.*, **43**, 802 (1997).

McCoy, B. J., and M. Wang, "Continuous-Mixture Fragmentation Kinetics: Particie Size Reduction and Molecular Cracking," *Chem. Eng. Sci.*, **49**, 3773 (1994).

McCoy, B. J., "Continuous Kinetics of Cracking Reactions: Thermolysis and Pyrolisis," *Chem. Eng. Sci.*, **51**, 2903 (1996).

Nace, D. M., S. E. Voltz, and V. W. Weekman, "Application of a Kinetic Model for Catalytic Cracking," *Ind. Eng. Chem Proc. Des. Dev.*, **10**, 530 (1971).

Oliveira, L. L., "Estimação de Parâmetros e Avaliação de Modelos de Craqueamento Catalítico," MSc Thesis (in Portuguese), Univ. Federal do Rio de Janeiro, Brazil (1987).

Ozawa, Y., "The Structure of a Lumpable Monomolecular System for Reversible Chemical Reactions," *Ind. Eng. Chem. Fundam.*, **12**, 191 (1973).

Peixoto, F. C., and J. L. de Medeiros, "Modeling and Parameter Estimation in Reactive Continuous Mixtures: The Catalytic Cracking of Linear Alkanes: I," *Braz. J. Chem. Eng.*, **16**, 65 (1999a).

Peixoto, F. C., and J. L. de Medeiros, "Modeling and Parameter Estimation in Reactive Continuous Mixtures: The Catalytic Cracking of Linear Alkanes: II," *Braz. J. Chem. Eng.*, **19**, 229 (1999b).

Peixoto, F. C., "Explicit Perturbation Solution of a Mass Structured Cell Population Balance Model," *Hybrid Methods Eng.*, **1**, 419 (1999).

Peixoto, F. C., G. M. Platt, and F. L. P. Pessôa, "Vapor-Liquid Equilibria of Multi-Indexed Continuous Mixtures Using an Equation of State and Group Contribution Methods," *Chem. Eng. J.*, **77**, 179 (2000).

Prasad, G. N., C. V. Wittman, S. B. Agnew, and T. Sridhar, "Modeling of Coal Liquefation Kinetics Based on Reactions in Continuous Mixtures," *AIChE J.*, **32**, 1277 (1986).

Quann, R. J., and S. B. Jaffe, "Building Useful Models of Complex Reaction Systems in Petroleum Refining," *Chem. Eng. Sci.*, **51**, 1615 (1996).

Ramkrishna, D., "The Status of Population Balances," *Rev. Chem. Eng.*, **3**, 49 (1985).

Sachanen, A. N., *The Chemical Constituents of Petroleum*, Reinhold, New York, p. 289, 303 (1945).

Tsang, T. H., and A. Rao, "A Moving Finite Element Method for the Population Balance Equation," *Int. J. Numerical Methods in Fluids*, **10**, 753 (1990).

Van Nes, K., and H. A. Van Westen, *Aspects of the Constituents of Mineral Oils*, Elsevier, New York, p. 335 (1951).

Voorhies, A., "Carbon Formation in Catalytic Cracking," *Ind. Eng. Chem.*, **37**, 318 (1945).

Wang, J. M. M., and B. J. McCoy, "Continuous Kinetics for Thermal Degradation of Polymer in Solution," *AIChE J.*, **41**, 1521 (1995).

Wei, S., and J. C. W. Kuo, "A Lumping Analysis in Monomolecular Reaction Systems," *Ind. Eng. Chem Fundam.*, 8, 114 (1969).

Manuscript received Apr. 3, 2000, and revision received Sept. 1, 2000.